



Myeloid-derived suppressor cells attenuate the antitumor efficacy of radiopharmaceutical therapy using ^{90}Y -NM600 in combination with androgen deprivation therapy in murine prostate tumors

Anusha Muralidhar,¹ Reinier Hernandez,² Zachary S Morris ,³
Hansel Comas Rojas,⁴ Malick Bio Idrissou,⁴ Jamey P Weichert,²
Douglas G McNeel ⁵

To cite: Muralidhar A, Hernandez R, Morris ZS, *et al.* Myeloid-derived suppressor cells attenuate the antitumor efficacy of radiopharmaceutical therapy using ^{90}Y -NM600 in combination with androgen deprivation therapy in murine prostate tumors. *Journal for ImmunoTherapy of Cancer* 2024;**12**:e008760. doi:10.1136/jitc-2023-008760

► Additional supplemental material is published online only. To view, please visit the journal online (<https://doi.org/10.1136/jitc-2023-008760>).

Accepted 14 April 2024



© Author(s) (or their employer(s)) 2024. Re-use permitted under CC BY-NC. No commercial re-use. See rights and permissions. Published by BMJ.

For numbered affiliations see end of article.

Correspondence to

Dr Douglas G McNeel;
dm3@medicine.wisc.edu

ABSTRACT

Rationale Androgen deprivation therapy (ADT) is pivotal in treating recurrent prostate cancer and is often combined with external beam radiation therapy (EBRT) for localized disease. However, for metastatic castration-resistant prostate cancer, EBRT is typically only used in the palliative setting, because of the inability to radiate all sites of disease. Systemic radiation treatments that preferentially irradiate cancer cells, known as radiopharmaceutical therapy or targeted radionuclide therapy (TRT), have demonstrable benefits for treating metastatic prostate cancer. Here, we explored the use of a novel TRT, ^{90}Y -NM600, specifically in combination with ADT, in murine prostate tumor models.

Methods 6-week-old male FVB mice were implanted subcutaneously with Myc-CaP tumor cells and given a single intravenous injection of ^{90}Y -NM600, in combination with ADT (degarelix). The combination and sequence of administration were evaluated for effect on tumor growth and infiltrating immune populations were analyzed by flow cytometry. Sera were assessed to determine treatment effects on cytokine profiles.

Results ADT delivered prior to TRT (ADT→TRT) resulted in significantly greater antitumor response and overall survival than if delivered after TRT (TRT→ADT). Studies conducted in immunodeficient NRG mice failed to show a difference in treatment sequence, suggesting an immunological mechanism. Myeloid-derived suppressor cells (MDSCs) significantly accumulated in tumors following TRT→ADT treatment and retained immune suppressive function. However, CD4+ and CD8+ T cells with an activated and memory phenotype were more prevalent in the ADT→TRT group. Depletion of Gr1+MDSCs led to greater antitumor response following either treatment sequence. Chemotaxis assays suggested that tumor cells secreted chemokines that recruited MDSCs, notably CXCL1 and CXCL2. The use of a selective CXCR2 antagonist, reparixin, further improved antitumor responses and overall survival when used in tumor-bearing mice treated with TRT→ADT.

WHAT IS ALREADY KNOWN ON THIS TOPIC

⇒ Androgen deprivation can work synergistically with external beam radiation therapy to prolong time to progression and survival of patients with high-risk localized prostate cancer. The combination of androgen deprivation and systemic targeted radionuclide therapy, however, and the optimal sequence of this combination, has not been previously evaluated.

WHAT THIS STUDY ADDS

⇒ In murine models of prostate cancer, we demonstrate that there is a sequence preference to the delivery of androgen deprivation and targeted radionuclide therapy, and this is mediated by differences in T cells and myeloid cells within the tumor immune microenvironment. The antitumor efficacy of this combination was improved by the addition of agents that depleted or reduced the migration of Gr-1+myeloid-derived suppressor cells.

HOW THIS STUDY MIGHT AFFECT RESEARCH, PRACTICE OR POLICY

⇒ Targeted radionuclide therapies for human prostate cancer might be best used following androgen deprivation and with agents such as CXCR2 antagonists that can inhibit the migration of immunosuppressive myeloid cells.

Conclusion The combination of ADT and TRT improved antitumor responses in murine models of prostate cancer, however, this was dependent on the order of administration. This was found to be associated with one treatment sequence leading to an increase in infiltrating MDSCs. Combining treatment with a CXCR2 antagonist improved the antitumor effect of this combination, suggesting a possible approach for treating advanced human prostate cancer.

BACKGROUND

Radiation therapy (RT) has been one of the mainstay treatments for prostate cancer. External beam RT (EBRT) can be curative for localized prostate cancer but has traditionally been limited to palliation for widely metastatic disease due to the inability to radiate all sites of metastasis.¹ Systemic administration of radionuclides that are preferentially taken up in bone has been used to treat painful bone metastases. These radionuclides include beta-emitting ⁸⁹Sr and ¹⁵³Sm, and US Food and Drug Administration (FDA)-approved alpha-emitting ²²³RaCl₂ (Xofigo) for the treatment of metastatic castration resistant prostate cancer (mCRPC) with bone metastases.^{2–4} This approach, using targeted radionuclides to treat all metastatic diseases simultaneously, with relative sparing of healthy tissue, is called radiopharmaceutical therapy or targeted radionuclide therapy (TRT).

While these TRT agents have been useful for patients with disease metastasized exclusively to the bone, they are not effective for those with other disease sites. Hence, other investigations have focused on compounds that specifically target cancer cells rather than the bone. One of the most studied targets for prostate tumor-directed radiation delivery is prostate-specific membrane antigen (PSMA) which is highly expressed in prostate cancer cells. Early attempts used ¹⁷⁷Lu or ⁹⁰Y conjugated to an antibody specific for PSMA (J591), which was well tolerated and promising in early clinical trials.^{5–6} Further efforts focused on the development of small molecules such as [¹⁸F]DCFPyL and PSMA-11, which have both been used in positron emission tomography (PET)/CT diagnostic imaging.^{7–8} Another PSMA analog, PSMA-617, has also been labeled with radionuclides suitable for therapy (eg, ¹⁷⁷Lu, ²²⁵Ac) of recurrent prostate cancer.⁹ ¹⁷⁷Lu-PSMA-617 was the first cancer-targeted TRT agent that received FDA approval for the treatment of mCRPC on the basis of it demonstrating a survival benefit compared with standard of care androgen receptor-targeted therapy, although by only 4 months.¹⁰

While androgen deprivation therapy (ADT) and RT are standard treatments for localized prostate cancer, there has been relatively limited exploration of ADT combined specifically with TRT.¹¹ Apart from their independent cytotoxic effects, there is evidence to suggest that ADT synergistically works with RT by preventing DNA repair.^{12–13} However, the order in which ADT and TRT are best administered has not been rigorously studied.¹⁴ Recent data indicate that RT and ADT can distinctly influence the tumor immune microenvironment.¹⁵ ADT enhances vulnerability to CD8+T cell-mediated destruction, triggers thymus regeneration, amplifies naive T cell production, augments immune cell infiltration from myeloid and lymphocyte populations, and elevates antibody responses against prostate-specific antigens.^{16–20} However, ADT also triggers a significant secretion of IL-8 in human prostate tumors, which can lead to the accumulation of intratumoral myeloid-derived suppressor cells (MDSCs), which may impede T-cell activity.²¹ Conversely,

RT elicits inflammatory responses, including the upregulation of MHC-I expression on tumor cells, enhancement of antigen cross-presentation by antigen-presenting cells, activation of the Fas/Fas ligand (Fas-L) signaling pathway, targeting of immune-suppressive populations like regulatory T cells (Tregs), and the induction of immunogenic cell death.^{22–23} In combination, ADT and RT can synergistically enhance tumor immunity, modulating both local and systemic antitumor immune responses.²⁴ Therefore, investigating effective strategies for their combination, including considerations such as the timing and sequence of ADT with RT, as well as the integration of newer systemic TRT agents, is crucial.

Our group has employed alkylphosphocholines (APCs) as TRT agents given that they can specifically accumulate within tumor cells by integrating into lipid rafts.²⁵ First-generation ¹³¹I-NM404 is currently under investigation as a potential monotherapy treatment for metastatic multiple myeloma and other cancer types.^{26–28} We have recently focused on the assessment of a second-generation APC chelate, called NM600, which can be tagged with different radiometals. By employing the radiometal ⁸⁶Y, one can visualize tumors and perform dosimetry measurements by PET/CT imaging.²⁹ Alternatively, through labeling with the isotopic pair, ⁹⁰Y, one can administer therapeutic radiation.^{30–31} This innovative approach, using Y-NM600 for both imaging and therapy, has demonstrated success in numerous preclinical models.^{29–30–32} However, its applicability to prostate cancer used in conjunction with ADT has not been previously investigated.

In this report, we explored the combination of TRT using ⁹⁰Y-NM600 with ADT in murine prostate models and specifically examined the effects of this combination on the tumor immune microenvironment. Our findings revealed that the effectiveness of this combination was influenced by the order of administration. ADT followed by TRT (ADT→TRT) showed superior enhancement of antitumor responses compared with the reverse sequence of TRT followed by ADT (TRT→ADT). We demonstrated that this disparity was due, in part, to the presence of infiltrating MDSCs, which impaired the function of CD8+T cells. Furthermore, we showed that the efficacy of antitumor responses could be improved by inhibiting the migration of MDSCs in vivo using a CXCR2 antagonist. These findings underscore the significance of understanding the mechanisms through which ADT and TRT influence the tumor microenvironment, enabling the optimal timing and choice of combination therapies for prostate cancer.

MATERIALS AND METHODS

Radiosynthesis of ⁹⁰Y-NM600

Cell lines

TRAMP-C1 (CRL-2730) and Myc-CaP (CRL-3255) cell lines were obtained from ATCC (Manassas, Virginia, USA), maintained according to ATCC recommendations, and tested for mycoplasma contamination.

Mice

FVB/NJ mice (stock #001800) and C57BL/6J mice (stock #000664) were obtained from The Jackson Laboratory (Bar Harbor, Maine, USA) and housed in micro insulator cages under aseptic conditions. NRG mice were graciously provided by Dr. Paul Sondel (University of Wisconsin-Madison). All animal studies were conducted under an IACUC-approved protocol.

Tumor implantation and tumor growth studies

1×10^6 Myc-CaP cells, resuspended in PBS, were implanted subcutaneously into the right flank of male FVB mice aged 4–6 weeks old or male NRG mice aged 6–10 weeks old. Similarly, wild-type male C57BL/6J mice aged 4–6 weeks were injected subcutaneously with 1×10^6 TRAMP-C1 cells in 1:1 ratio in phosphate buffered saline (PBS): Matrigel (Corning, NY, CB354248) into the right flank. 12–15 days postinjection, when tumors were palpable and similarly sized (0.2 – 0.3 cm^3), mice were randomized into treatment groups. Tumors were measured twice weekly via calipers until the tumors reached 2 cm^3 . Tumor volumes were calculated as $(\text{long axis} \times \text{short axis}^2) / 2$.

Androgen deprivation therapy

Mice were treated subcutaneously with either degarelix (25 mg/kg) or a vehicle sham treatment (PBS) every 28 days starting when the tumor volume reached ~ 0.2 – 0.3 cm^3 in size.

Radiosynthesis of $^{86/90}\text{Y-NM600}$

Briefly, $^{86}\text{YCl}_3$ was provided by the University of Wisconsin-Madison cyclotron group after proton bombardment of enriched [^{86}Sr] SrCO_3 solid targets in a PETtrace biomedical cyclotron and elution of ^{86}Y from a diglycolamide extraction resin column.³³ Clinical grade $^{90}\text{YCl}_3$ and NM600 were obtained from PerkinElmer (Shelton, CT) and Archeus Technologies (Madison, WI) respectively. NM600 was radiolabeled with ^{90}Y or ^{86}Y and purified as previously described.^{29, 30} Briefly, 185 – 370 MBq (5 – 10 mCi) of $^{86/90}\text{Y}$ was buffered with 0.1 M NaOAc (pH 5.5) and mixed with 55 – 110 nmol (50 – $100 \mu\text{g}$). The reaction was incubated for 30 min at 95°C under constant shaking (500 rpm). $^{86/90}\text{Y-NM600}$ was purified by a solid-phase extraction cartridge (HLB; Waters) and eluted in 2 mL of 200-proof ethanol. The eluate was then evaporated and dried under a nitrogen stream, and $^{86/90}\text{Y-NM600}$ was reconstituted in excipient (saline containing 0.1% v/v Tween20). Radiochemical yield was assessed by instant thin-layer chromatography (iTLC) using silica-impregnated paper as the stationary phase and run using 50 mM ethylenediaminetetraacetic acid, which moves the free radiometals with the solvent front ($R_f=1$) while $^{86/90}\text{Y-NM600}$ remains at the origin ($R_f=0$). iTLC chromatograms were developed using a cyclone phosphor-plate imager and analyzed with Optiquant software (PerkinElmer). Radiochemical purity and stability were determined via radiolabeled high-performance liquid chromatography (HPLC) using a reverse-phase $250 \times 3.00 \text{ mm}$ C18 Luna

$5 \mu\text{m}$ 100 \AA column (Phenomenex) and a water:acetonitrile gradient (5% MeCN: 0 – 2 min ; 5% – 65% MeCN: 2 – 30 min ; 65% – 90% MeCN: 30 – 35 min ; 90% – 5% MeCN: 35 – 45 min). The final radiochemical purity obtained consistently surpassed 95% with an average molar specific activity of $18 \text{ GBq}/\mu\text{mol}$ for both $^{90}\text{Y-NM600}$ and $^{86}\text{Y-NM600}$ ($n>5$). Additionally, HPLC chromatograms indicated that both $^{90}\text{Y-NM600}$ and $^{86}\text{Y-NM600}$ were stable in mouse serum over at least 48 hours.²⁹

Dosimetry estimation

Dosimetry estimations were performed as previously reported using a Monte Carlo-based dosimetry assessment platform, Radionuclide Assessment Platform for Internal Dosimetry.^{34, 35} The dosimetry and biodistribution of $^{90}\text{Y-NM600}$ have been previously published for murine Myc-CaP and TRAMP-C1 prostate tumors.^{29, 32}

TRT administration

$^{90}\text{Y-NM600}$ $250 \mu\text{Ci}$ – 9.25 MBq was injected into the tail vein of tumor-bearing mice 1 week before or after the start of ADT. Based on dosimetry studies, a single dose of $250 \mu\text{Ci}$ injected activity delivered 5 – 6 Gy absorbed dose to TRAMP-C1 tumors and 16 – 20 Gy to Myc-CaP tumors.^{29, 32}

Antibody treatments

All antibody treatments, anti-CD4 (BioXcell BP0003-1), anti-CD8 (BioXcell BP0061) and IgG2a isotype (BioXcell BP0085), were administered as $200 \mu\text{g}$ intraperitoneal injections, on days 2, 4, and 6 post-ADT or TRT. $200 \mu\text{g}$ anti-mouse Gr-1 antibody (clone RB6-8C5) (BD Pharmingen 552985) was administered intraperitoneally three times a week post-TRT administration.

Flow cytometry

Tumors were collected at different time points, then digested for 1–2 hours at 37°C in mouse cell culture medium: RPMI 1640 with L-glutamine, 10% fetal calf serum, 200 U/mL Pen/Strep, 5% sodium pyruvate, 5% HEPES, and $50 \mu\text{M}$ β -MeOH supplemented with 2 mg/mL collagenase, 0.2 mg/mL DNase I, and 1 tablet protease inhibitor (Sigma-Aldrich, St. Louis, MO, 11697498001) per 50 mL digest solution. Digests were then passed through $100 \mu\text{m}$ screens. 5×10^6 cells were plated and Fc blocked (BD, Franklin Lakes, NJ, 553142) for 20 min at 4°C . Cells were then stained for 30 min at 4°C with the viability dye Ghost Dye Red 780 (Tonbo 13-0865T100) and the following antibodies: CD11b-BB515 (BD 564454), CD25-BB700 (BD 566498), GR-1-PE-CF594 (BD 562710), CD3-PE-Cy7 (eBiosciences Thermo Fisher Scientific, Waltham, MA 25-0031-82), MHCII-BV421 (Biolegend San Diego, CA 107632), CD45-BV510 (BD 563891), CD4-BV605 (Biolegend 100451), CD19-BV711 (BD 563157), CD11c-APC (BD 550261), CD8-AF700 (100730), CD44-AF488 (Biolegend 103016), CD45-PerCP-Cy5.5 (Biolegend 103132), KLRG-1-PE (Biolegend 138408), CD69-PE-CF594 (BD 562455), CD62L-BV510 (Biolegend 104441), CD103-BV605 (Biolegend 121453), CD27-BV785 (Biolegend 124241), CD4-APC-Cy7 (Biolegend

561830). Cells were then fixed and permeabilized with the eBiosciences Foxp3/Transcription Factor Staining Buffer Set overnight at 4°C (Thermo Fisher 00-5523-00). Cells were then stained with intracellular antibodies for 30 min at 4°C: FoxP3-PE (Thermo Fisher 12-5773-82), Ki67-BV421 (BD 562899). Flow cytometry was performed on a Thermo Fisher Attune NxT cytometer and data were analyzed using FlowJo V.10. Gates were set according to a fluorescence-minus-one control. Flow cytometry data were reported as either the percentage of populations among all CD45+ events or as a frequency per gm of tumor tissue.

CXCR2 antagonist

CXCR2 antagonist, reparixin (Selleckchem, Houston, Texas), was reconstituted in Tween-80 and PBS in a 1:4 ratio and administered subcutaneously at 5 mg/kg on the left flank thrice a week for 3 weeks post-TRT administration.

In vitro studies

CD8 T cell suppression assay

Spleens were harvested from naïve FVB mice and passed through 100 µm screens. CD8+T cells were isolated from splenocytes via immunomagnetic negative selection (StemCell #19853), and then labeled with carboxyfluorescein succinimidyl ester (Biolegend #423801) according to the manufacturer's instructions. Tumors were collected from treated tumor-bearing mice on day 36, processed into single-cell suspensions as above, and CD11b+Gr-1+Ly-6G+MDSCs were isolated (Miltenyi Biotec #130-094-538). 1×10^5 labeled CD8+T cells were cultured together with MDSCs at a 1:1 ratio. CD8+T cells were stimulated with anti-CD3/anti-CD28 coated beads (Thermo Fisher 11 456D) at a ratio of 2 beads per CD8+T cell. Cells were cultured with 30 units/mL of human IL-2 for 72 hours in 96-well plates before analysis via flow cytometry.

ELISA

ELISA was performed as previously described.³⁶ Briefly, Immulon plates (Thermo Fisher, Waltham, Massachusetts, USA) were coated with anti-mouse IFN γ antibody (BD #551216) and incubated overnight at 4°C. Plate were then blocked with PBS/1% BSA before adding standards (BD #554587) or cell culture supernatants and incubated overnight at 4°C. The next day, a biotin-conjugated anti-mouse IFN γ antibody was added (BD #554410), followed by avidin-HRP (BioRad Hercules, CA, 170-6528). TMB Substrate (Kirkegaard and Perry, Gaithersburg, MD, 50-76-01) was added and OD was measured at 450 nm.

Luminex assay

50 µL of sera or conditioned media from in vitro assays was evaluated for 26 different cytokines and chemokines using the Cytokine & Chemokine 26-Plex Mouse ProcartaPlex Panel 1 (Thermo Fisher EPX260-26088-901) according to the manufacturer's instructions. The plate was read on a Luminex MagPix instrument. Analytes were divided according to their type, Th1 (IFN gamma,

IL-12p70, IL-18, IL-27, IL-2, TNF alpha, GMCSF, IL-1 beta), Th2 (IL-4, IL-5, IL-6, IL-9, IL-10, IL-13, GMCSF), Th17 (IL-17A, IL-22, IL-23), and chemokines (CXCL10, CXCL1, CCL2, CCL7, CCL3, CCL4, CXCL2, CCL5, CCL11).

In vitro chemotaxis assay

3×10^5 cells (Myc-CaP cells and/or T cells including CD4 and CD8 T cells isolated from naïve FVB mice splenocytes) were plated in regular media, charcoal-stripped media (regular media with charcoal-stripped FBS (Thermo#12676029), ⁹⁰Y containing media (23.3 µCi~0.86 MBq of ⁹⁰Y per 1 mL media) or ⁹⁰Y-containing charcoal-stripped media, in 6-well plates (n=3 replicates per media condition). Wells containing T cells were stimulated with anti-CD3/anti-CD28 coated beads at a ratio of 2 beads per CD8+T cell. Supernatants were collected after incubation for 72 hours. 1×10^5 MDSCs isolated from tumors as described above were added to the top chamber of the transwell and cultured for 12 hours with the conditioned media in the bottom well. In related experiments, a 5 ng/mL recombinant CXCL1 was used as a positive control, and MDSCs were pretreated with 4 mM reparixin. In other related experiments, conditioned media from T cells were added to the Myc-CaP conditioned media in a 1:1 ratio. After incubation, cells were collected from the bottom well, stained, and analyzed via flow cytometry. The absolute number of MDSCs was determined and the percent migration was calculated as the fraction of MDSCs present in the bottom well of the total number of MDSCs plated in the transwell.

Statistical analysis

Tumor growth data, comparing group means among treatment groups, were analyzed by fitting a linear mixed-effects model with Geisser-Greenhouse correction. The data were analyzed via analysis of variance followed by Tukey's multiple-comparison test. Survival analysis was conducted using a Mantel-Cox log-rank test. For all comparisons, p values ≤ 0.05 were considered statistically significant with asterisks *p<0.05, **p<0.01, and ***p<0.001. All statistical analyses were performed using GraphPad Prism software V.10.0.3.

RESULTS

Combination of ADT and TRT with ADT prior to TRT (ADT→TRT) significantly improved antitumor responses in murine prostate tumor models

We studied the effects of ⁹⁰Y-NM600 in combination with ADT in two separate murine prostate tumor models, Myc-CaP and TRAMP-C1. As depicted in figure 1A, Myc-CaP tumor cells were implanted subcutaneously in male FVB mice, and when tumors reached a volume of 0.2–0.3 cm³ they were treated with degarelix. TRT (250 µCi~9.25 MBq of ⁹⁰Y-NM600, delivering~16 Gy) was given 1 week before or after degarelix. When ADT was delivered prior to TRT (ADT→TRT), there was a significant tumor growth

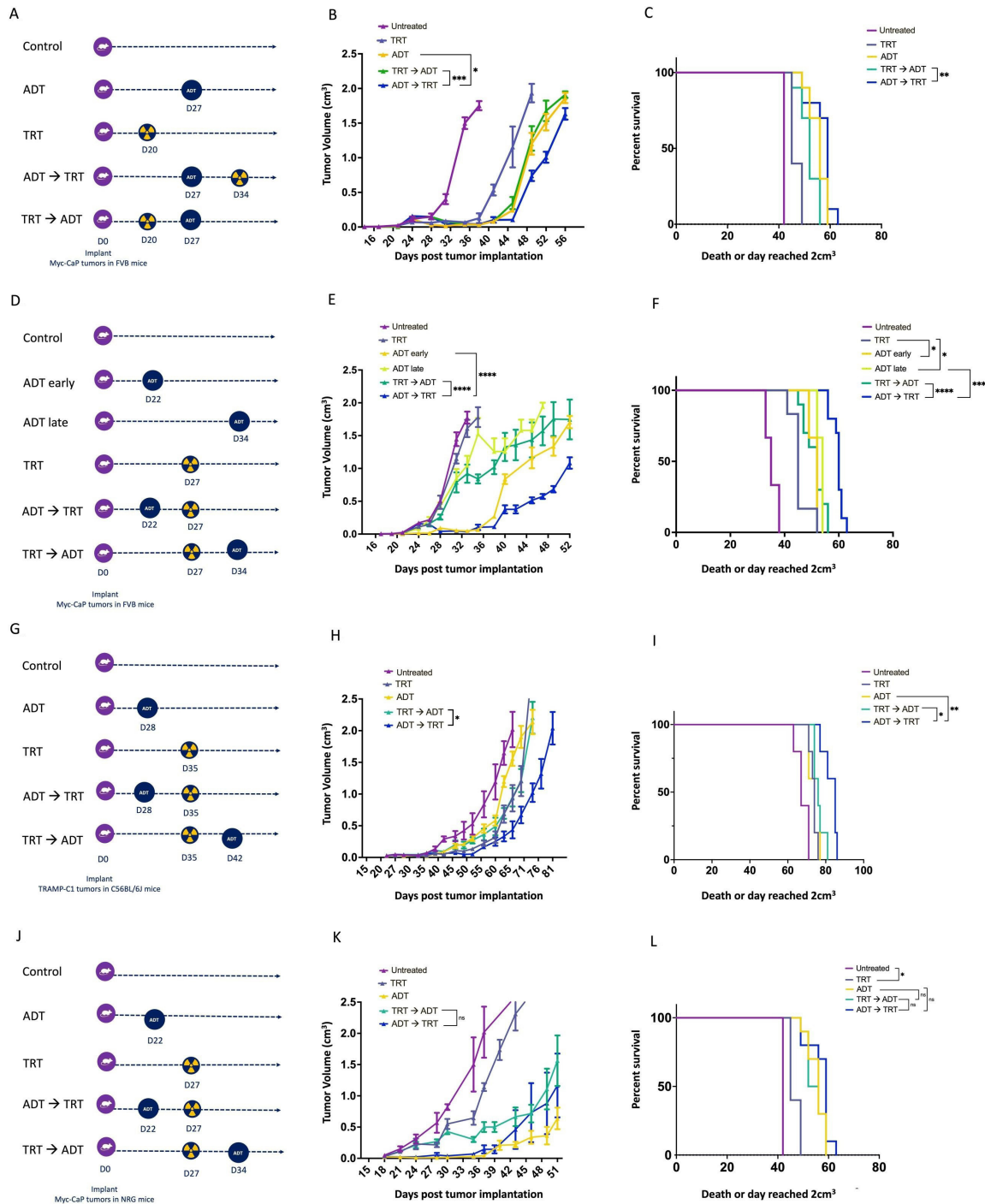


Figure 1 Combination of ADT and TRT with ADT prior to TRT (ADT→TRT) significantly improved antitumor responses in murine prostate tumor models. FVB mice were implanted with Myc-CaP tumor cells and treated with degarelix (ADT), with TRT delivered before or after ADT, and followed for tumor growth (n=10 per group). Shown is a schema (A), tumor growth curves (B), and Kaplan-Meier curves depicting survival (time to a tumor size of 2 cm³ or death, C). A similar study fixed the day of TRT with ADT delivered before or after (n=10 per group). Shown is the schema (D), tumor growth curves (E), and Kaplan-Meier survival curves (time to tumor size of 2 cm³ or death, F). Similarly, male C57BL/6 mice were implanted with TRAMP-C1 tumor cells (n=5 per group) and treated with ADT delivered before or after TRT. Shown is the schema (G), tumor growth curves (H), and Kaplan-Meier survival curves (time to tumor size of 2 cm³ or death, I). In addition, Myc-CaP tumor cells were implanted in male NRG T-cell deficient mice, treated with ADT and/or TRT as before (n=10 per group), and followed for tumor growth (schema in J). Shown are the tumor growth curves (K) and Kaplan-Meier survival curves (L). For tumor growth curves, asterisks demonstrate significant (*p<0.05, **p<0.01, ***p<0.001, ****p<0.0001) differences as assessed by linear mixed effects model with Geisser-Greenhouse correction and Tukey's multiple comparisons test with individual variances; Kaplan-Meier curves were compared using the log-rank test with asterisks indicating *p<0.05, **p<0.01, ***p<0.001, ****p<0.0001. Results are from one experiment and are representative of two independent experiments for each study (online supplemental figure 2). ADT, androgen deprivation therapy; TRT, targeted radionuclide therapy.

delay (figure 1B and online supplemental figure 1A) and improved overall survival (figure 1C). Because ADT and TRT can have different effects depending on the day they are administered relative to tumor volume, in a second study, ADT was again used before or after TRT, but this time fixing the day on which TRT was administered (figure 1D). As before, the ADT→TRT combination significantly delayed tumor growth (figure 1E and online supplemental figure 1B and 2) and improved overall survival (figure 1F) compared with the monotherapies or TRT→ADT combination. ADT→TRT also significantly improved antitumor responses and overall survival in a prostate tumor model in which TRAMP-C1 tumor cells were implanted in C57BL/6 mice (figure 1G–I and online supplemental figure 1C). However, there was no evidence of improved treatment response or overall survival when Myc-CaP cells were implanted in NRG mice lacking functional T cells (figure 1J–L and online supplemental figure 1D). Overall, these findings demonstrated that ADT and TRT had a stronger antitumor effect in combination and were dependent on the order of administration, with ADT→TRT leading to superior antitumor responses, and this was likely immune cell dependent.

CD4+T and CD8+T cells persisted in the tumor microenvironment in the ADT→TRT sequence whereas significant increases in MDSCs were observed in the TRT→ADT sequence

We next sought to understand the effect of sequencing these treatments on the tumor immune microenvironment. A similar study was performed as in figure 1D, but tumors were collected at several time points following treatment for evaluation of immune cell compositions via flow cytometry, as shown in figure 2A. Representative flow plots for T cells and MDSCs are shown in figure 2B (and gating strategy shown in online supplemental figure 3). We found that CD4+T and CD8+T cells persisted in the tumor microenvironment until day 32 in the ADT→TRT treated mice (figure 2C,D) compared with the TRT→ADT treated mice (figure 2E,F, and online supplemental figure 4). Increases in MDSCs were not observed in ADT→TRT mice until day 39, and there were no significant changes in regulatory CD4+T cells following treatment (figure 2G,H). Notably, MDSCs were significantly increased in the TRT→ADT group immediately after TRT treatment and this increase was further accentuated with the subsequent administration of ADT (figure 2I), whereas there were no significant changes in regulatory CD4+T cells (figure 2J). Taken together, these data suggested that the balance of CD4+T cells, CD8+T cells and MDSC affected by these treatments might have contributed to the preferred treatment sequence.

ADT→TRT led to persistence of activated and memory CD8+ T cells while these were significantly reduced in the TRT→ADT group

A similar study was performed to further characterize CD8+T cells (figure 3A) (with the gating strategy shown in

online supplemental figure 5). Tumor-infiltrating CD8+T cells from mice treated in the ADT→TRT sequence were found to have increased proliferation (Ki67+) and activation (CD69) (figure 3B,C) compared with the TRT→ADT treatment sequence (figure 3D,E). Notably, memory CD8+T cells in the ADT→TRT sequence persisted, including effector and resident memory populations (figure 3F, G, J and K). Conversely, the TRT→ADT sequence led to a significant reduction in memory CD8+T cells, notably effector and resident memory populations (figure 3H, I, L and M). In summary, these findings indicate that the ADT→TRT treatment sequence facilitated the sustained presence of activated and memory CD8+T cells, whereas these populations were substantially diminished in mice initially treated with TRT.

T cell depletion reduces the antitumor efficacy of the combination of ADT and TRT

We next sought to understand if T cells were required in mediating differences in antitumor responses by depleting these populations immediately after ADT or TRT (figure 4A). In the ADT→TRT group, depleting CD4+T or CD8+T cells resulted in a slightly accelerated tumor growth, although the difference was not statistically significant. However, in the TRT→ADT group, CD8+T cell depletion led to significantly more rapid tumor growth (figure 4B and online supplemental figure 6). Regardless of the combination sequence, depletion of T cells worsened survival (figure 4C).

MDSC depletion significantly improved antitumor responses and increased infiltration of CD4+ and CD8+ T cells into prostate tumors

We next wished to determine whether tumor infiltrating MDSCs that were present following TRT were functionally immunosuppressive. MDSCs were obtained from mice treated with TRT with or without ADT and evaluated for their effects on CD8+T cell proliferation (figure 5A). We found that MDSCs obtained from tumors of mice treated with TRT alone had a slight suppressive effect on CD8+T cell proliferation, however, MDSCs from mice subjected to the TRT→ADT treatment markedly suppressed CD8+T cell proliferation (figure 5B). MDSC from mice treated with either TRT alone or TRT→ADT similarly suppressed IFN γ secretion from CD8+T cells stimulated with anti-CD3/anti-CD28 beads (figure 5C). These data demonstrate that MDSCs infiltrating tumors in mice treated with TRT were still functionally active. We next used clodronate liposomes or anti-Gr1 antibody to deplete these myeloid populations in mice treated with TRT→ADT (figure 5D). Either of these treatments resulted in significantly greater tumor control compared with control mice (figure 5E and online supplemental figure 7). These treatments led to a significant decrease in tumor-infiltrating MDSCs (figure 5F), as well as slight

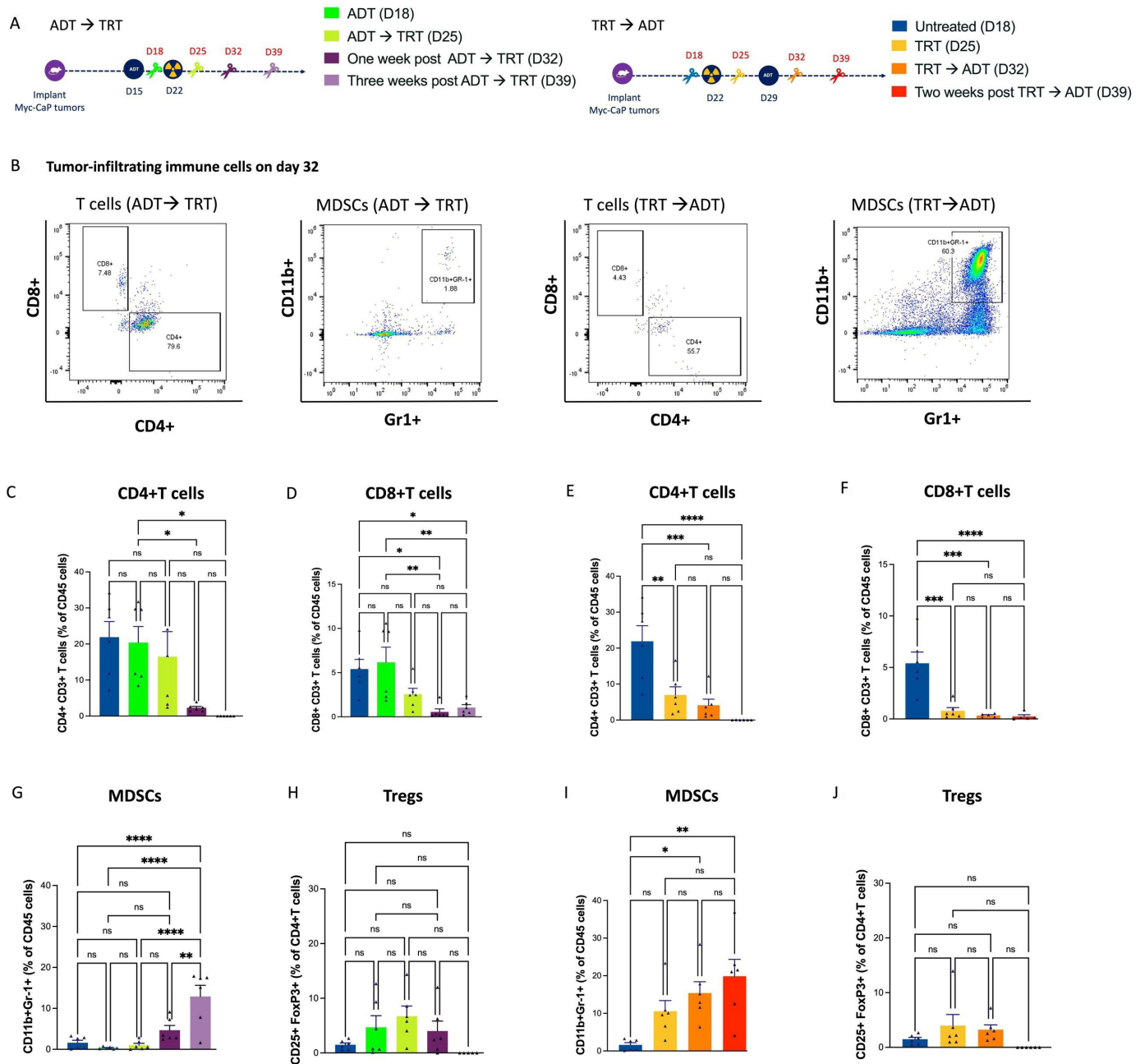


Figure 2 CD4+T and CD8+T cells persist in the tumor microenvironment in the ADT→TRT sequence combination whereas significant increases in MDSCs were observed in the TRT→ADT sequence. Myc-CaP tumor cells were implanted in male FVB mice and treated with ADT and/or TRT, with tumors sampled at different days for flow cytometry analysis (n=6 per group per time point). Shown are a schema (A) and representative dot plots (B) of CD4+CD3+ and CD8+CD3+ T cells and CD11b+Gr1+ MDSCs in ADT→TRT (left panels) and TRT→ADT groups (right panels) collected on day 32. CD4+T cells (C, E), CD8+T cells (D, F), and CD11b+Gr-1+ MDSC (G, I) are shown as a percentage of CD45+ cells. CD4+FoxP3+ Treg (H, J) are shown as a percentage of CD4+ cells. C–J were compared using one-way ANOVA with Tukey's multiple comparisons test asterisks indicating *p<0.05, **p<0.01, ***p<0.001, ****p<0.0001. Results are from one experiment and are representative of two independent experiments (online supplemental figure 4). ADT, androgen deprivation therapy; ANOVA, analysis of variance; MDSCs, myeloid-derived suppressor cells; TRT, targeted radionuclide therapy.

increases in tumor-infiltrating CD4+ (figure 5G) and CD8+ (figure 5H) T cells.

Cytokines and chemokines secreted by tumor cells promote MDSC infiltration into tumors

We next explored the potential mechanism of tumor infiltration by MDSCs by investigating the effects of the

combination treatments on the cytokines and chemokines present in the sera following these different treatments (figure 6A and online supplemental figure 8). As shown in figure 6B–F, CXCL1, CXCL2 and CCL5, all chemokines associated with myeloid cell migration, were significantly increased in sera

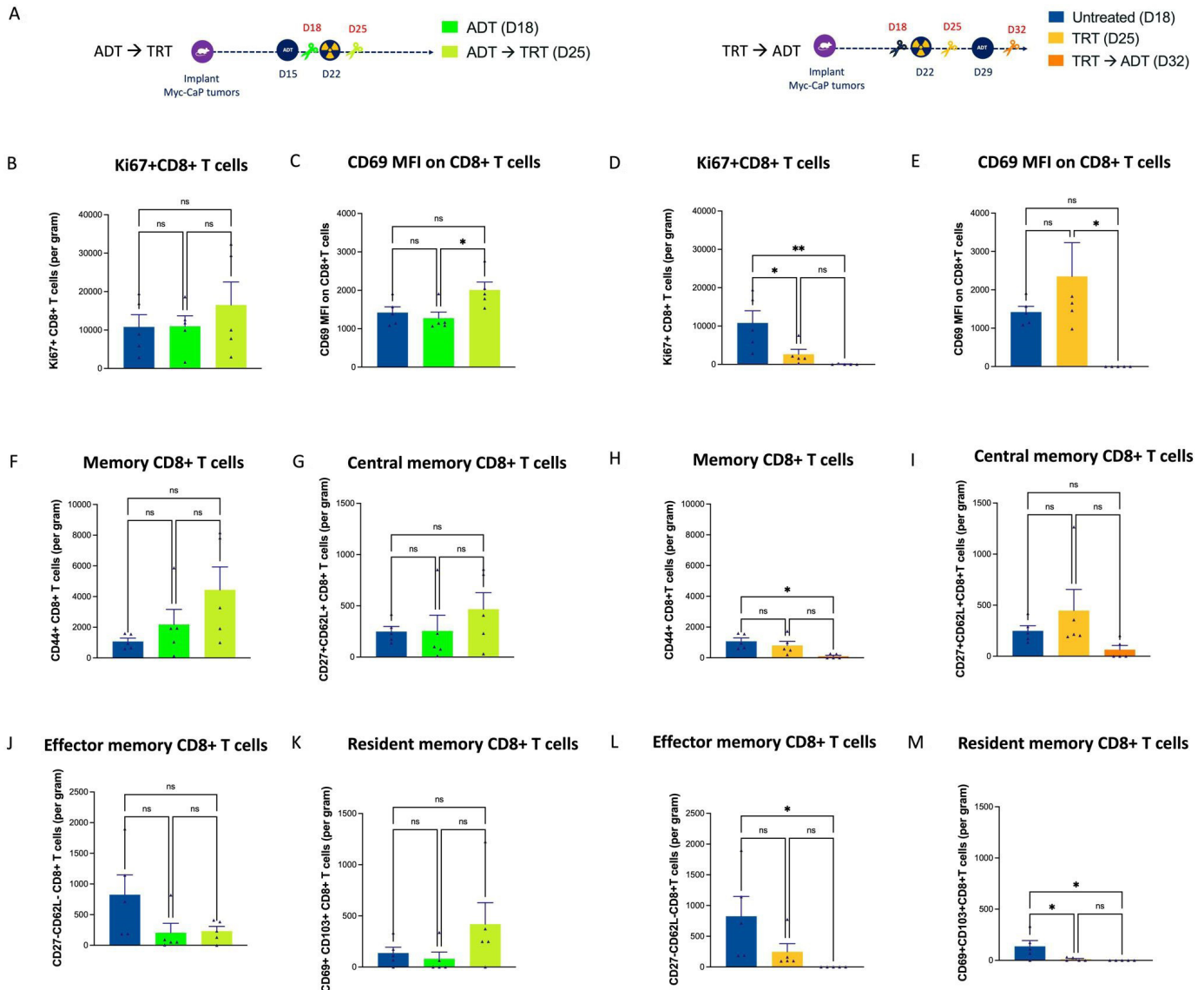


Figure 3 ADT→TRT led to persistence of activated and memory CD8+T cells while these were significantly reduced in the TRT→ADT group. Myc-CaP tumor cells were implanted in male FVB mice, treated with ADT and/or TRT as before, and tumors were sampled at different days (n=5 per group per time point) for flow cytometry analysis of CD8+CD3+ cells (schema in A). Untreated CD8+T cells were collected from animals on day 18. Left panels indicate data from ADT→TRT treated animals, and right panels indicate data from TRT→ADT treated animals. Data indicate the number of each population per gram of tumor for Ki67+CD8+CD3+ T cells (B and D), CD69 MFI on CD8+T cells (C, E), CD44+ memory CD8+ T cells (F, H), CD44+CD27+CD62L+ central memory CD8+T cells (G and I), CD44+CD27-CD62L- effector memory CD8+T cells (J, L), and CD69+CD103+ resident memory CD8+T cells (K, M). Comparisons were made using one-way ANOVA with Tukey's multiple comparisons test asterisks indicating *p<0.05, **p<0.01. Results are from one experiment and are representative of two independent experiments. ADT, androgen deprivation therapy; ANOVA, analysis of variance; TRT, targeted radionuclide therapy.

of mice treated with the TRT→ADT sequence relative to the ADT→TRT sequence. To determine which cell types may be involved in MDSC recruitment, a chemotaxis assay was performed using tumor cells, T cells, or the combination, in a testosterone-replete or testosterone-deficient medium (figure 6G). As shown in figure 6H, tumor cells primarily contributed to MDSC migration. The presence of T cells slightly reduced the migration of MDSC. Similar differences were observed using testosterone replete or testosterone-deficient medium media containing ^{90}Y

(online supplemental figure 9A). CXCL1 and CXCL2 were increased significantly in Myc-CaP conditioned media (figure 6I,J) while CCL2, CCL3, CCL5 were increased in conditioned media containing Myc-CaP and T cells (figure 6K-M). No significant changes were observed in other chemokines and cytokines (online supplemental figures 9B and 10).

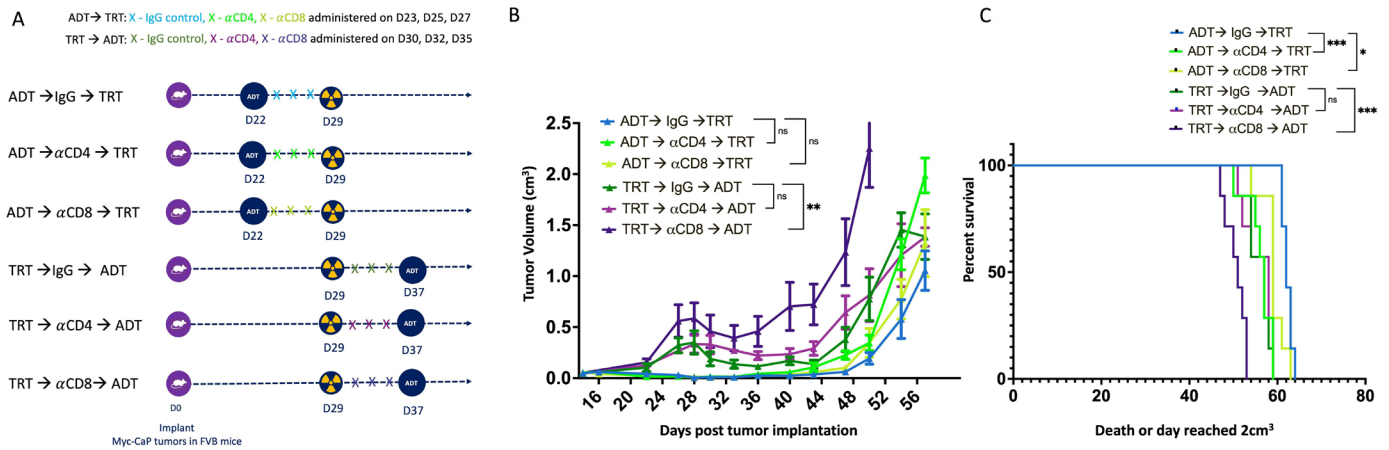


Figure 4 The antitumor efficacy of the combination of ADT and TRT worsened in the absence of T cells. Myc-CaP tumor cells were implanted in male FVB mice, treated with ADT and/or TRT as before, and mice received IgG, anti-CD4 or anti-CD8 depleting antibodies between these treatments (schema in A). Shown are the tumor growth curves (B) and Kaplan-Meier survival curves (C). For tumor growth curves, comparisons were made by linear mixed effects model with Geisser-Greenhouse correction and Tukey's multiple comparisons test with individual variance; Kaplan-Meier curves were compared using the log-rank test. Asterisks demonstrate significant differences (* $p < 0.05$, ** $p < 0.01$, *** $p < 0.001$). Results shown are each from one experiment ($n = 7$ per group). ADT, androgen deprivation therapy; TRT, targeted radionuclide therapy.

CXCR2 blockade improves antitumor efficacy in the TRT → ADT combination

Because tumor cells appeared primarily responsible for MDSC recruitment, and MDSC recruitment was inhibited in the presence of T cells, this suggested that CXCL1 and CXCL2 produced by tumor cells may be the dominant chemokines involved in MDSC recruitment. Consequently, we next tested if CXCL1 directly contributed to MDSC migration in vitro, and whether this might be affected by blockade of the CXCL1/CXCL2 receptor, CXCR2 (figure 7A). As demonstrated in figure 7B, we observed that MDSCs exhibited a migratory response toward supernatants containing CXCL1, and this response was significantly reduced when CXCR2 was blocked using reparixin. We next wanted to determine whether blocking CXCR2 could improve the antitumor response of the TRT → ADT treatment sequence (figure 7C). As demonstrated in figure 7D and online supplemental figure 11, mice treated with reparixin showed improved antitumor responses. Tumors from these mice exhibited a significant reduction in MDSCs (figure 7E), a slight increase in CD4+T cells (figure 7F), and a significant increase in CD8+T cells (figure 7G). Similar improved antitumor responses were found in mice treated with ADT → TRT and reparixin (online supplemental figure 12).

DISCUSSION

Following the approval of ^{177}Lu -PSMA-617, there has been a growing interest in the utilization of TRT for the treatment of prostate cancer, either as a standalone therapy or in combination with other treatments. However, there is currently a lack of preclinical data that can provide insights into how TRT affects immune cell populations within tumors and

how it can be optimally integrated with other immunomodulatory treatments. This report is the first combining TRT using ^{90}Y -NM600 with ADT in immune competent murine prostate tumor models, with an emphasis on investigating the effects of immune modulation and the critical aspects of timing and sequence in this combination therapy approach. Our primary findings can be summarized as follows: (1) Administering ADT → TRT yielded significant advantages compared with the reverse sequence, as demonstrated by both a delayed time to tumor growth and improved overall survival; (2) ADT → TRT was associated with the sustained presence of activated and memory CD8+T cells within the tumor microenvironment; (3) TRT → ADT group exhibited increased infiltration of MDSCs that were functionally active in suppressing CD8+T cell function; and (4) inhibiting CXCR2, the receptor for CXCL1 and CXCL2, effectively inhibited the migration of MDSCs and improved the antitumor response with TRT → ADT. The observed outcomes highlight the crucial role of the administration sequence of ADT and TRT in modulating the tumor immune microenvironment, thereby influencing therapeutic responses. Moreover, the identification of molecular targets, exemplified by CXCR2 blockade, offers mechanistic insights to guide novel approaches aimed at enhancing treatment outcomes.

The combination of ADT and RT is a standard treatment regimen for localized prostate cancer, supported by evidence from trials such as reported by Bolla, which demonstrated improved survival for patients with high-risk prostate cancer treated with RT and androgen deprivation compared with RT alone.³⁷ Despite the established efficacy of this combined approach, a lingering controversy surrounds the optimal timing and sequence for administering ADT and RT. Individual trials have suggested a similar advantage in progression-free survival using ADT prior to and concurrent (neoadjuvant ADT) with EBRT, rather than concurrent

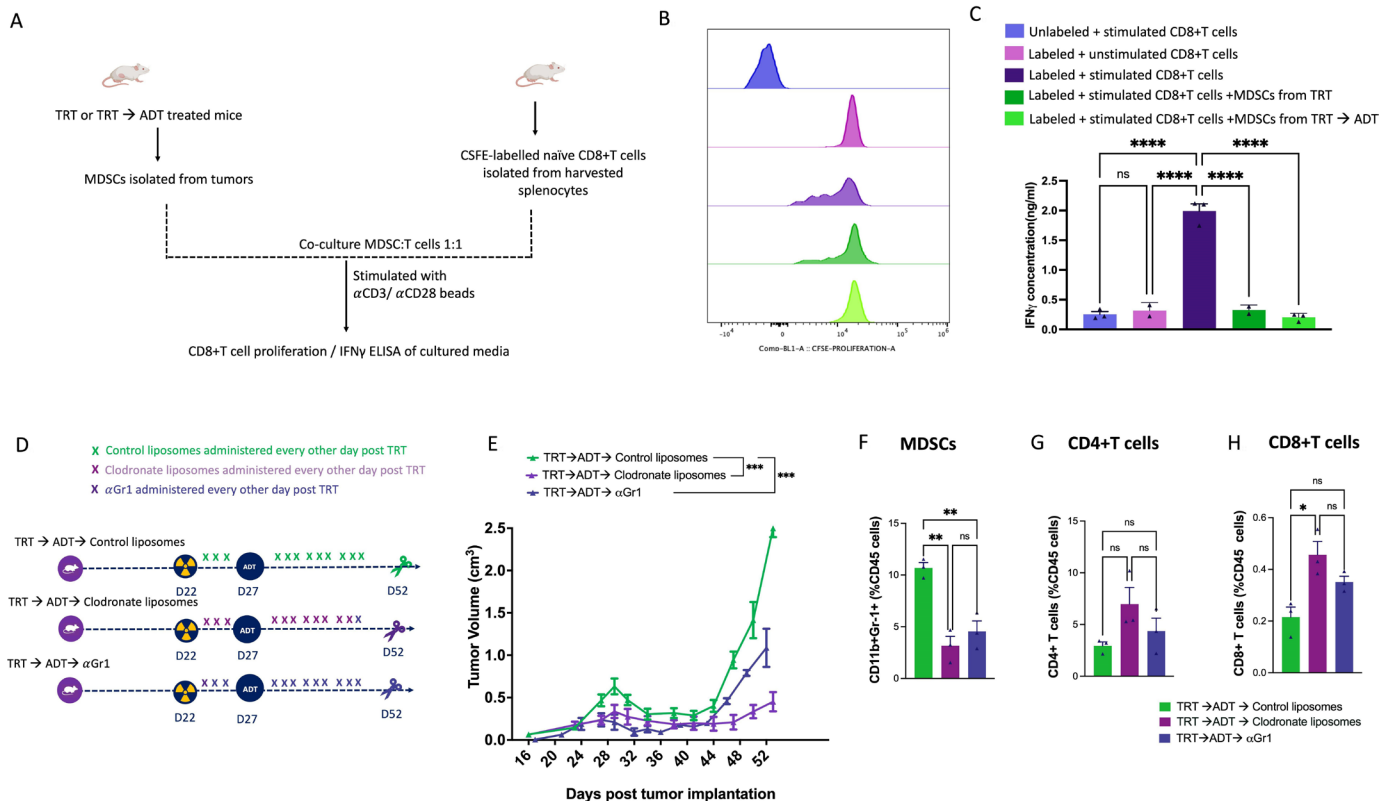


Figure 5 Depletion of MDSCs significantly improved antitumor responses and increased infiltration of CD4+ and CD8+ T cells into prostate tumors. CD11b+Gr-1+ MDSC were collected from Myc-CaP tumor-bearing mice that had been treated with TRT alone or TRT→ADT. MDSCs were cocultured with naïve, CFSE-labeled CD8+T cells and stimulated with anti-CD3/anti-CD28 beads (schema in A). After 72 hours, flow cytometry was conducted to evaluate CD8+T cell proliferation by loss of CFSE (B), and culture supernatants were evaluated for IFN γ concentration (C). Myc-CaP tumor cells were implanted in male FVB mice, treated with TRT→ADT as before, and mice received control liposomes, clodronate liposomes, (n=7 per group) or anti-Gr-1 antibody (n=3) as indicated (schema in D). Shown are the tumor growth curves (E). Tumors were collected on day 54 (n=3 per group) and evaluated by flow cytometry for CD11b+Gr-1+ MDSC (F), CD4+T cells (G), and CD8+T cells (H). For tumor growth curves, asterisks demonstrate significant (p<0.05) differences as assessed by linear mixed effects model with Geisser-Greenhouse correction. For F–H, comparisons were made using one-way ANOVA with Tukey’s multiple comparisons test; asterisks indicate *p<0.05, **p<0.01, ***p<0.001, ****p<0.0001. Results are from one experiment, and representative of results from an independent experiment (online supplemental figure 7B). ADT, androgen deprivation therapy; ANOVA, analysis of variance; CFSE, carboxyfluorescein succinimidyl ester; MDSCs, myeloid-derived suppressor cells; TRT, targeted radionuclide therapy.

and following EBRT (adjuvant ADT), such as the Radiation Therapy Oncology Group 94134 trial.³⁸ A more recent similar trial, however, showed no difference in outcome between these similar approaches.³⁹ A pooled meta-analysis of 12 randomized trials, however, found that concurrent/adjuvant ADT was associated with improved metastasis-free survival and overall survival compared with patients receiving neoadjuvant/concurrent ADT, at least for patients receiving prostate-only EBRT, compared with patients who received larger field RT.⁴⁰ The time frames of treatment over days in our study to treatment over the course of months in these clinical trials are certainly different and may account for differences in sequence preference. Notwithstanding, the potential impacts of ADT and EBRT on the tumor immune microenvironment have been underappreciated as a potential mechanism for differences observed in clinical trials, particularly since differences were observed if regional lymph nodes were included in the radiation fields.

The investigation into the combined effects of ADT and RT has primarily focused on potential synergies arising from direct cytotoxic effects and the induction of increased DNA damage.⁴¹ However, what remains significantly underexplored is the interplay of these therapies with immune cells within the tumor microenvironment. There is a general consensus that tumor-infiltrating lymphocytes (TILs) have a role in detecting and eradicating tumor cells, and their presence is linked to improved patient outcomes.⁴² More specifically, CD8+T cells correlated with enhanced 5-year overall survival in patients undergoing radical prostatectomy (98% vs 91%, p=0.01) and prostate cancer-specific survival (99% vs 95%, p=0.04) compared with individuals exhibiting low CD8+TIL density.⁴³ Our studies substantiate this observation, demonstrating that enhanced overall survival is associated with increased CD8+T cells in the ADT→TRT sequence. Interestingly, while the use of TRT clearly led to a decrease in tumor-infiltrating T cells in either treatment sequence,

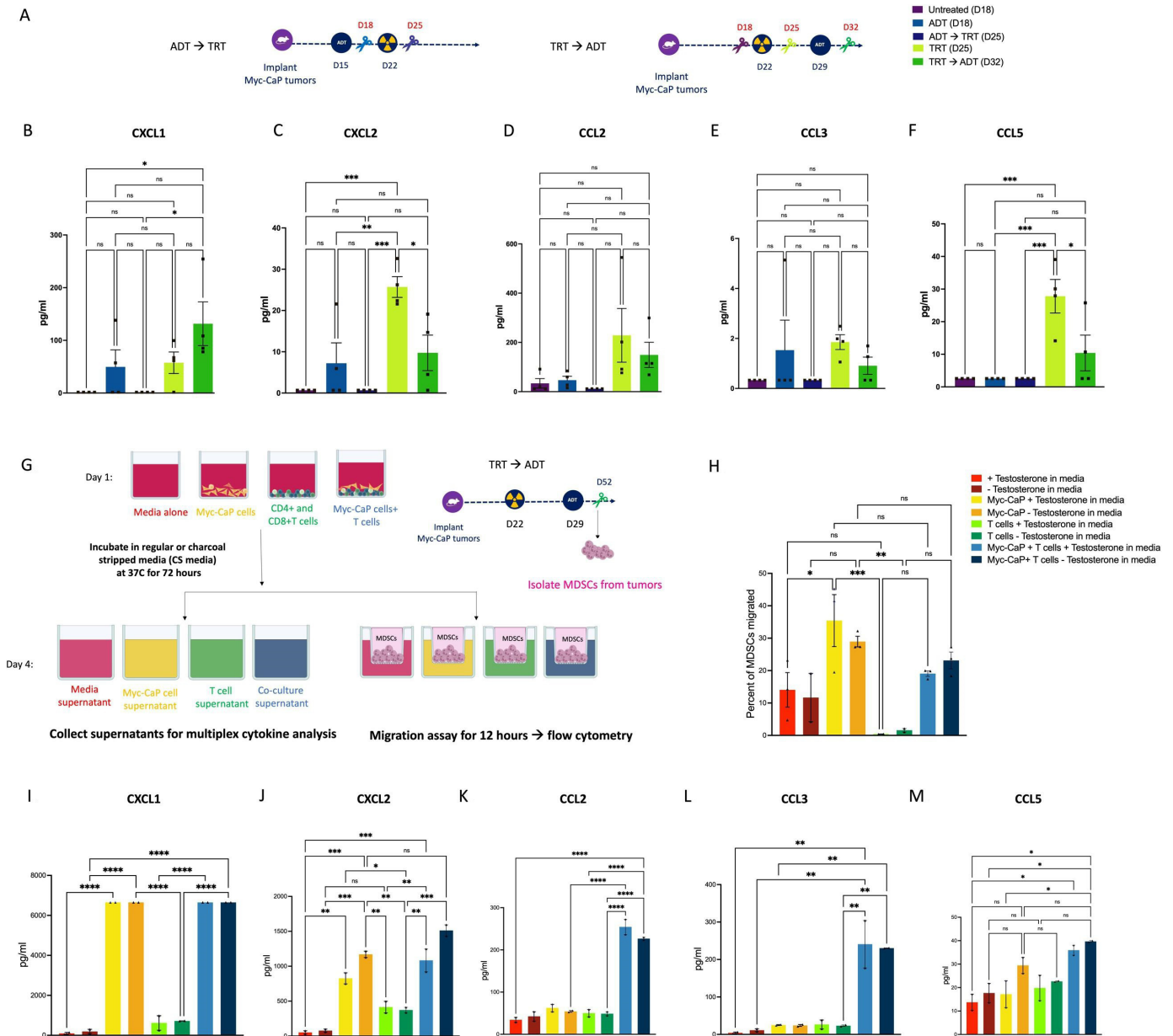


Figure 6 Cytokines and chemokines secreted by tumor cells promote MDSC infiltration into tumors. Myc-CaP tumor cells were implanted in male FVB mice, treated with ADT and/or TRT as before, and sera were collected at different days ($n=2$ per group per time point) for cytokine and chemokine quantification (schema in A). Shown are concentrations of cytokines in pg/mL for CXCL1 (B), CXCL2 (C), CCL2 (D), CCL3 (E), and CCL5 (F). Culture supernatant from cultured Myc-CaP cells, naïve CD4+ and CD8+ T cells, the combination, or media alone (containing testosterone-replete or testosterone-deficient serum) were placed in the bottom of transwell chambers, with MDSC collected from treated mice placed in the upper chambers (schema in G). The percentage of MDSC that migrated to the bottom chamber was determined by flow cytometry (H), and the conditioned media were evaluated for CXCL1 (I), CXCL2 (J), CCL2 (K), CCL3 (L), and CCL5 (M). B–F and H–M were compared using one-way ANOVA with Tukey’s multiple comparisons test with asterisks indicating $*p<0.05$, $**p<0.01$, $***p<0.001$, $****p<0.0001$. Results are from one experiment with $n=3$ per condition and are representative of two independent experiments. ADT, androgen deprivation therapy; ANOVA, analysis of variance; MDSC, myeloid-derived suppressor cell; TRT, targeted radionuclide therapy.

as expected since T cells are relatively sensitive to radiation, there were still more tumor-infiltrating T cells when ADT was used prior to TRT. Others have demonstrated that ADT alone can lead to an increase in tumor-infiltrating CD4+ and CD8+ T cells.^{16 44} We expect this is due to release of chemokines recruiting T cells following ADT. Conceivably, the use of TRT, in addition to depleting tissue-resident T cells, may have also disrupted the release of these chemokines, leading to this

observed difference due to treatment sequence. This will be an area for future studies.

Clinical data indicate that the accumulation of MDSCs in the bloodstream of patients with advanced prostate cancer, and an intratumoral myeloid signature, are linked to unfavorable outcomes.⁴⁵ Various strategies have been investigated to target MDSCs, encompassing efforts to deplete MDSCs, hinder their function by inhibiting immunosuppressive

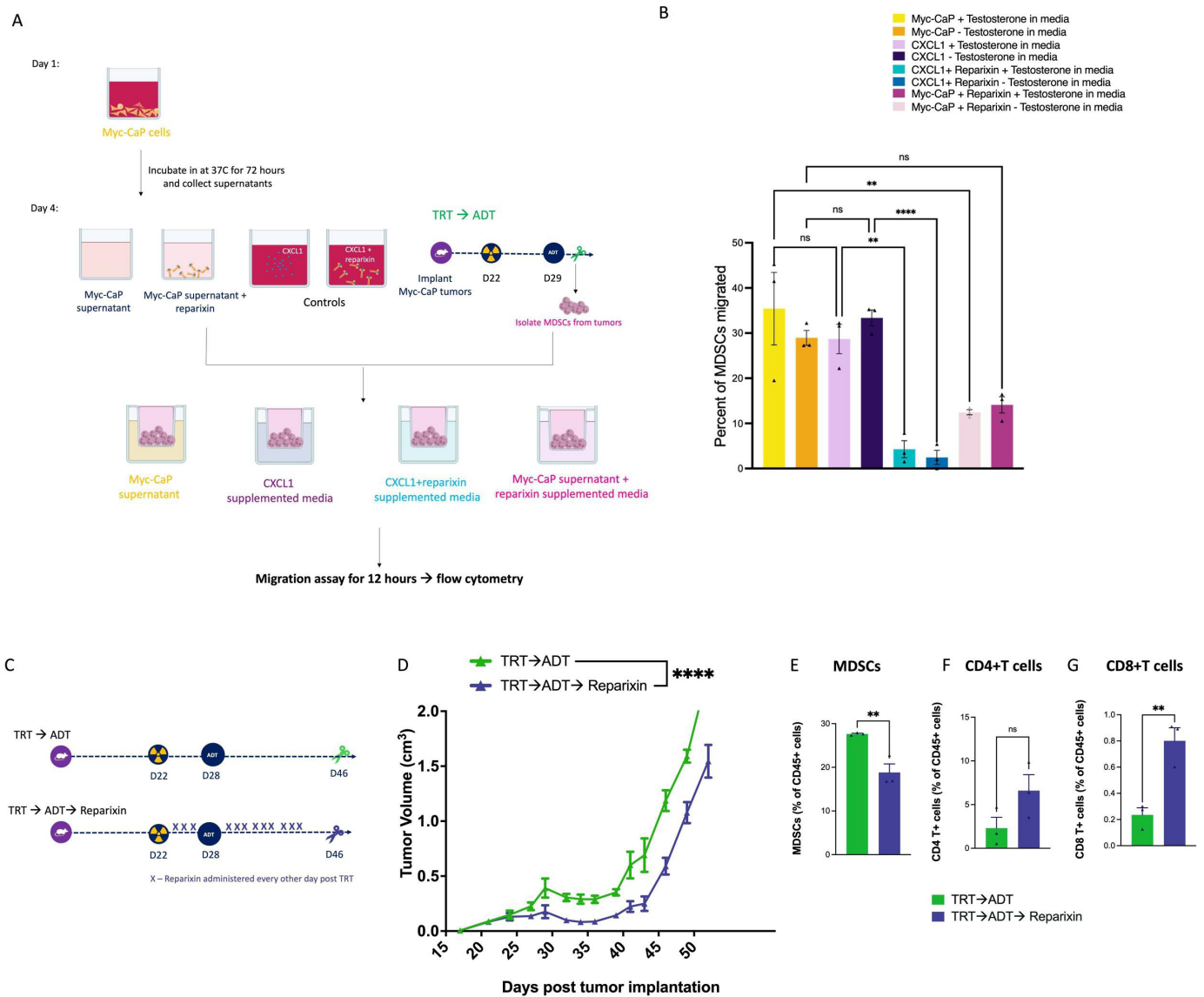


Figure 7 CXCR2 blockade improves antitumor efficacy in the TRT→ADT combination. Culture supernatant from cultured Myc-CaP cells, with or without naïve CD4+ and CD8+ T cells, and with or without CXCL1 or reparixin, were placed in the bottom of transwell chambers, with MDSC collected from treated mice placed in the upper chambers with n=3 per condition (schema in A). MDSC migration was determined after 12 hours (B). Myc-CaP tumor cells were implanted in male FVB mice (n=7 mice per group), treated with TRT→ADT as before, and then treated with reparixin or vehicle as indicated (schema in C). Shown are the tumor growth curves (D). Tumors were collected on day 46 (n=3 from each group) and evaluated by flow cytometry for CD11b+Gr-1+ MDSC (E), CD4+T cells (F), and CD8+T cells (G). For tumor growth curves, differences were assessed by linear mixed effects model with Geisser-Greenhouse correction. Conditions in B were compared using one-way ANOVA with Tukey's multiple comparisons test and E–G were compared using unpaired-t tests. Asterisks indicate **p<0.01, ****p<0.0001. Results shown are each from one experiment. ADT, androgen deprivation therapy; ANOVA, analysis of variance; MDSC, myeloid-derived suppressor cell; TRT, targeted radionuclide therapy.

mediators, and induce their maturation to stimulate differentiation.⁴⁶ Efforts to therapeutically target myeloid cells broadly have thus far failed clinically, potentially due to myeloid cell heterogeneity and complexity. Targeting the recruitment of MDSCs has been explored through the inhibition of various chemokines and chemokine receptors, such as the use of CSF-1R antibody, but these approaches have demonstrated limited success in clinical trials.^{47,48} Currently, blockade of IL-8, which interacts with the CXCR2 receptor typically secreted by prostate cancer cells, is undergoing testing in a phase Ib/

II clinical trial (NCT03689699). It is important to note that IL-8 is naturally absent in mice, suggesting that mice rely on alternative chemokines, notably CXCL1 and CXCL2, to facilitate MDSC recruitment.^{21,49} Recent studies have shown that CXCL1 can influence the differentiation and function of MDSCs by promoting the expansion of MDSCs in the tumor microenvironment, contributing to immune suppression and facilitating tumor progression.⁵⁰ In addition, CXCL1 can also enhance the suppressive activity of MDSCs, further exacerbating their immunosuppressive effects. Therefore,

targeting CXCR2 and its effects on MDSCs may represent a promising therapeutic approach for cancer and other inflammatory diseases.⁵¹ Clinical trials evaluating the efficacy of reparixin, either alone or in combination with other treatments, have been initiated in patients with metastatic breast cancer.⁵² In addition to its effects on MDSCs, reparixin also has anti-inflammatory properties and can modulate the function of other immune cells, such as neutrophils and macrophages.^{53–54} Thus, selectively blocking chemokine activity emerges as an attractive therapeutic strategy to increase tumor cell sensitivity to immune-modulating treatments. The CXCR2 inhibitor navarixin, which has been used in clinical trials for chronic obstructive pulmonary diseases with established safety and toxicity profiles,⁵⁵ is now also under evaluation in a clinical trial (NCT03473925) for its efficacy in treating advanced prostate cancer.

In conclusion, our study advances the understanding of the interplay between ADT, TRT, and the immune micro-environment in prostate cancer. The sequence-dependent effects on immune populations and treatment resistance emphasize the need for meticulous optimization of treatment timing and sequencing. Tailoring treatment strategies to harness these immunological dynamics represents a promising avenue for further improving therapeutic outcomes in advanced prostate cancer. We anticipate that the exploration of TRT combined with ADT, as well as other immune modulating agents, will remain an active focus in both preclinical and clinical investigations for prostate cancer, notably given the relatively recent approval of ¹⁷⁷Lu-PSMA-617 and the evaluation of other TRT agents for advanced prostate cancer. In future studies, we plan to specifically evaluate ¹⁷⁷Lu-PSMA-617 in murine models of prostate cancer that express PSMA, to determine if there is a similar sequence-dependent effect on immune populations when that agent is used in combination with ADT. In addition, the use of immune checkpoint inhibitors is actively being pursued in combination with TRT (eg, NCT03805594, NCT03658447). Based on our results presented here, future studies should also evaluate the additional use of ADT in combination with immune checkpoint inhibition and TRT.

Author affiliations

¹Oncology, University of Wisconsin-Madison, Madison, Wisconsin, USA

²Radiology, University of Wisconsin-Madison, Madison, Wisconsin, USA

³Human Oncology, University of Wisconsin Madison School of Medicine and Public Health, Madison, Wisconsin, USA

⁴Department of Medical Physics, University of Wisconsin-Madison, Madison, Wisconsin, USA

⁵Medicine, University of Wisconsin-Madison, Madison, Wisconsin, USA

Acknowledgements We thank Justin Jeffrey, Ashley Weichmann and Zack Rosenkrans for assistance with administration of NM600 to animals. We thank the staff of the University of Wisconsin Flow Cytometry Core Facility, and for helpful communication and assistance provided by Dr Hemanth Potluri and Ms Daeun Shim.

Contributors AM wrote the manuscript, performed all experiments, and carried out data analysis. RH, ZSM, and JPW assisted in the experimental design. HCR and MBI prepared the 90Y-NM600 agent. DGM oversaw the experimental design, edited the manuscript and is responsible for the overall content as the guarantor. All authors approved of the final manuscript.

Funding This project was supported, in part, through the NIH National Cancer Institute (NCI) grant P01CA250972.

Disclaimer The content is solely the responsibility of the authors and does not necessarily represent the official views of the NIH.

Competing interests JPW is a co-founder and Senior Science Advisor for Archeus Technologies, which holds the license rights to NM600-related technologies. ZSM and RH have financial interest in Archeus Technologies. HCR has served as a consultant for Archeus Technologies. ZSM is a member of the Scientific Advisory Boards for Archeus Technologies, Seneca Therapeutics, and NorthStar Medical Isotopes. ZSM is an inventor on patents or filed patents managed by the Wisconsin Alumni Research Foundation relating to immunotherapies and the interaction of targeted radionuclide therapies and immunotherapies. The other authors have no relevant potential conflicts of interest.

Patient consent for publication Not applicable.

Ethics approval Study protocols involving animals (M005690) were reviewed and approved by the University of Wisconsin Institutional Animal Care and Use Committee.

Provenance and peer review Not commissioned; externally peer reviewed.

Data availability statement Data are available on reasonable request. The data generated and/or analyzed during this study are available from the corresponding author on reasonable request.

Supplemental material This content has been supplied by the author(s). It has not been vetted by BMJ Publishing Group Limited (BMJ) and may not have been peer-reviewed. Any opinions or recommendations discussed are solely those of the author(s) and are not endorsed by BMJ. BMJ disclaims all liability and responsibility arising from any reliance placed on the content. Where the content includes any translated material, BMJ does not warrant the accuracy and reliability of the translations (including but not limited to local regulations, clinical guidelines, terminology, drug names and drug dosages), and is not responsible for any error and/or omissions arising from translation and adaptation or otherwise.

Open access This is an open access article distributed in accordance with the Creative Commons Attribution Non Commercial (CC BY-NC 4.0) license, which permits others to distribute, remix, adapt, build upon this work non-commercially, and license their derivative works on different terms, provided the original work is properly cited, appropriate credit is given, any changes made indicated, and the use is non-commercial. See <http://creativecommons.org/licenses/by-nc/4.0/>.

ORCID iDs

Zachary S Morris <http://orcid.org/0000-0001-5558-3547>

Douglas G McNeel <http://orcid.org/0000-0003-1471-6723>

REFERENCES

- Rusthoven CG, Jones BL, Flaig TW, *et al.* Improved survival with prostate radiation in addition to androgen deprivation therapy for men with newly diagnosed metastatic prostate cancer. *J Clin Oncol* 2016;34:2835–42.
- Sartor O, Reid RH, Hoskin PJ, *et al.* Samarium-153-Lexidronam complex for treatment of painful bone metastases in hormone-refractory prostate cancer. *Urology* 2004;63:940–5.
- Strontium-89 for palliation of pain from bone metastases in patients with prostate and breast cancer - PubMed. 2023. Available: <https://pubmed.ncbi.nlm.nih.gov/9323260/>
- Hoskin P, Sartor O, O'Sullivan JM, *et al.* Efficacy and safety of radium-223 dichloride in patients with castration-resistant prostate cancer and symptomatic bone metastases, with or without previous docetaxel use: a prespecified subgroup analysis from the randomised, double-blind, phase 3 ALSYMPCA trial. *Lancet Oncology* 2014;15:1397–406.
- Bander NH, Milowsky MI, Nanus DM, *et al.* Phase I trial of ¹⁷⁷Lutetium-labeled J591, a monoclonal antibody to prostate-specific membrane antigen, in patients with androgen-independent prostate cancer. *JCO* 2005;23:4591–601.
- Tagawa ST, Milowsky MI, Morris M, *et al.* Phase II study of Lutetium-177-labeled anti-prostate-specific membrane antigen monoclonal antibody J591 for metastatic castration-resistant prostate cancer. *Clin Cancer Res* 2013;19:5182–91.
- Morris MJ, Rowe SP, Gorin MA, *et al.* Diagnostic performance of 18F-Dcfpyl-PET/CT in men with biochemically recurrent prostate cancer: results from the CONDOR phase III, multicenter study. *Clin Cancer Res* 2021;27:3674–82.

- 8 Pienta KJ, Gorin MA, Rowe SP, *et al.* A phase 2/3 prospective multicenter study of the diagnostic accuracy of prostate specific membrane antigen PET/CT with ¹⁸F-Dcfpyl in prostate cancer patients (OSPREY). *J Urol* 2021;206:52–61.
- 9 Eder M, Schäfer M, Bauder-Wüst U, *et al.* 68Ga-complex lipophilicity and the targeting property of a urea-based PSMA inhibitor for PET imaging. *Bioconjug Chem* 2012;23:688–97.
- 10 Sartor O, de Bono J, Chi KN, *et al.* Lutetium-177-PSMA-617 for metastatic castration-resistant prostate cancer. *N Engl J Med* 2021;385:1091–103.
- 11 Coulter JB, Song DY, DeWeese TL, *et al.* Mechanisms, challenges, and opportunities in combined radiation and hormonal therapies. *Semin Radiat Oncol* 2022;32:76–81.
- 12 Polkinghorn WR, Parker JS, Lee MX, *et al.* Androgen receptor signaling regulates DNA repair in prostate cancers. *Cancer Discov* 2013;3:1245–53.
- 13 Sekhar KR, Wang J, Freeman ML, *et al.* Radiosensitization by enzalutamide for human prostate cancer is mediated through the DNA damage repair pathway. *PLoS ONE* 2019;14:e0214670.
- 14 Dal Pra A, Cury FL, Souhami L. Combining radiation therapy and androgen deprivation for localized prostate cancer—a critical review. *Curr Oncol* 2010;17:28–38.
- 15 Wang C, Zhang Y, Gao W-Q. The evolving role of immune cells in prostate cancer. *Cancer Lett* 2022;525:9–21.
- 16 Long X, Hou H, Wang X, *et al.* Immune signature driven by ADT-induced immune microenvironment remodeling in prostate cancer is correlated with recurrence-free survival and immune infiltration. *Cell Death Dis* 2020;11:779.
- 17 Qin C, Wang J, Du Y, *et al.* Immunosuppressive environment in response to androgen deprivation treatment in prostate cancer. *Front Endocrinol* 2022;13:1055826.
- 18 Tang S, Moore ML, Grayson JM, *et al.* Increased Cd8+ T-cell function following Castration and immunization is countered by parallel expansion of regulatory T cells. *Cancer Res* 2012;72:1975–85.
- 19 Roden AC, Moser MT, Tri SD, *et al.* Augmentation of T cell levels and responses induced by androgen deprivation. *J Immunol* 2004;173:6098–108.
- 20 Gamat M, McNeel DG. Androgen deprivation and immunotherapy for the treatment of prostate cancer. *Endocr Relat Cancer* 2017;24:T297–310.
- 21 Lopez-Bujanda ZA, Haffner MC, Chaimowitz MG, *et al.* Castration-mediated IL-8 promotes myeloid infiltration and prostate cancer progression. *Nat Cancer* 2021;2:803–18.
- 22 Lee Y, Auh SL, Wang Y, *et al.* Therapeutic effects of ablative radiation on local tumor require Cd8+ T cells: changing strategies for cancer treatment. *Blood* 2009;114:589–95.
- 23 Demaria S, Bhardwaj N, McBride WH, *et al.* Combining radiotherapy and immunotherapy: a revived partnership. *Int J Radiat Oncol Biol Phys* 2005;63:655–66.
- 24 Kalina JL, Neilson DS, Comber AP, *et al.* Immune modulation by androgen deprivation and radiation therapy: implications for prostate cancer immunotherapy. *Cancers (Basel)* 2017;9:13.
- 25 Weichert JP, Clark PA, Kandela IK, *et al.* Alkylphosphocholine analogs for broad-spectrum cancer imaging and therapy. *Sci Transl Med* 2014;6:240ra75.
- 26 Grudzinski JJ, Titz B, Kozak K, *et al.* A phase 1 study of 131I-Clr1404 in patients with relapsed or refractory advanced solid tumors: dosimetry, biodistribution, pharmacokinetics, and safety. *PLoS One* 2014;9:e111652.
- 27 Ailawadhi S, Stiff PJ, Ibrahim E, *et al.* Fractionated dosing of CLR 131 in patients with Relapsed or refractory multiple myeloma (RRMM). *Blood* 2019;134:144.
- 28 Lubner SJ, Mullvain J, Perlman S, *et al.* A phase 1, multi-center, open-label, dose-escalation study of 131I-Clr1404 in subjects with Relapsed or refractory advanced solid malignancies. *Cancer Invest* 2015;33:483–9.
- 29 Grudzinski JJ, Hernandez R, Marsh I, *et al.* Preclinical characterization of 86/90Y-Nm600 in a variety of murine and human cancer tumor models. *J Nucl Med* 2019;60:1622–8.
- 30 Hernandez R, Walker KL, Grudzinski JJ, *et al.* 90Y-Nm600 targeted radionuclide therapy induces immunologic memory in syngeneic models of T-cell non-Hodgkin's lymphoma. *Commun Biol* 2019;2:79.
- 31 Patel RB, Hernandez R, Carlson P, *et al.* Low-dose targeted radionuclide therapy renders immunologically cold tumors responsive to immune Checkpoint blockade. *Sci Transl Med* 2021;13:eabb3631.
- 32 Potluri HK, Ferreira CA, Grudzinski J, *et al.* Antitumor efficacy of 90 Y-Nm600 targeted radionuclide therapy and PD-1 blockade is limited by regulatory T cells in murine prostate tumors. *J Immunother Cancer* 2022;10:e005060.
- 33 Aluicio-Sarduy E, Hernandez R, Valdovinos HF, *et al.* Simplified and automatable radiochemical separation strategy for the production of radiopharmaceutical quality 86Y using single column extraction chromatography. *Appl Radiat Isot* 2018;142:28–31.
- 34 Besemer AE, Yang YM, Grudzinski JJ, *et al.* Development and validation of RAPID: a patient-specific Monte Carlo three-dimensional internal dosimetry platform. *Cancer Biother Radiopharm* 2018;33:155–65.
- 35 Bednarz B, Grudzinski J, Marsh I, *et al.* Murine-specific internal dosimetry for preclinical investigations of imaging and therapeutic agents. *Health Phys* 2018;114:450–9.
- 36 Johnson LE, Frye TP, Chinnasamy N, *et al.* Plasmid DNA vaccine encoding prostatic acid phosphatase is effective in eliciting autologous antigen-specific CD8+ T cells. *Cancer Immunol Immunother* 2007;56:885–95.
- 37 Bolla M, Van Tienhoven G, Warde P, *et al.* External irradiation with or without long-term androgen suppression for prostate cancer with high metastatic risk: 10-year results of an EORTC randomised study. *Lancet Oncol* 2010;11:1066–73.
- 38 Roach M, Moughan J, Lawton CAF, *et al.* Sequence of hormonal therapy and radiotherapy field size in unfavourable, localised prostate cancer (NRG/RTOG 9413): long-term results of a randomised, phase 3 trial. *Lancet Oncol* 2018;19:1504–15.
- 39 Malone S, Roy S, Eapen L, *et al.* Sequencing of androgen-deprivation therapy with external-beam radiotherapy in localized prostate cancer: a phase III randomized controlled trial. *J Clin Oncol* 2020;38:593–601.
- 40 Ma TM, Sun Y, Malone S, *et al.* Sequencing of androgen-deprivation therapy of short duration with radiotherapy for nonmetastatic prostate cancer (SANDSTORM): a pooled analysis of 12 randomized trials. *J Clin Oncol* 2023;41:881–92.
- 41 Wu C-T, Chen W-C, Chen M-F. The response of prostate cancer to androgen deprivation and irradiation due to immune modulation. *Cancers (Basel)* 2019;11:20.
- 42 Galon J, Costes A, Sanchez-Cabo F, *et al.* Type, density, and location of immune cells within human colorectal tumors predict clinical outcome. *Science* 2006;313:1960–4.
- 43 Yang Y, Attwood K, Bshara W, *et al.* High Intratumoral Cd8+ T-cell infiltration is associated with improved survival in prostate cancer patients undergoing radical Prostatectomy. *Prostate* 2021;81:20–8.
- 44 Gamat-Huber M, McNeel DG. Androgen deprivation as a tumour-Immunomodulating treatment. *Nat Rev Urol* 2020;17:371–2.
- 45 Bronte G, Conteduca V, Landriscina M, *et al.* Circulating myeloid-derived suppressor cells and survival in prostate cancer patients: systematic review and meta-analysis. *Prostate Cancer Prostatic Dis* 2023;26:41–6.
- 46 Koinis F, Xagara A, Chantzara E, *et al.* Myeloid-derived suppressor cells in prostate cancer: present knowledge and future perspectives. *Cells* 2021;11:20.
- 47 Autio KA, Klebanoff CA, Schaer D, *et al.* Immunomodulatory activity of a colony-stimulating Factor-1 receptor inhibitor in patients with advanced refractory breast or prostate cancer: A phase I study. *Clinical Cancer Research* 2020;26:5609–20.
- 48 Moeller A, Kurzrock R, Botta GP, *et al.* Challenges and prospects of CSF1R targeting for advanced malignancies. *Am J Cancer Res* 2023;13:3257–65.
- 49 Lee J, Cacalano G, Camerato T, *et al.* Chemokine binding and activities mediated by the mouse IL-8 receptor. *J Immunol* 1995;155:2158–64.
- 50 Shi H, Han X, Sun Y, *et al.* Chemokine (C-X-C motif) ligand 1 and CXCL2 produced by tumor promote the generation of Monocytic myeloid-derived suppressor cells. *Cancer Sci* 2018;109:3826–39.
- 51 Bullock K, Richmond A. Suppressing MDSC recruitment to the tumor Microenvironment by antagonizing Cxcr2 to enhance the efficacy of Immunotherapy. *Cancers (Basel)* 2021;13:6293.
- 52 Goldstein LJ, Mansutti M, Levy C, *et al.* A randomized, placebo-controlled phase 2 study of paclitaxel in combination with reparixin compared to paclitaxel alone as front-line therapy for metastatic triple-negative breast cancer (fRida). *Breast Cancer Res Treat* 2021;190:265–75.
- 53 Alfaro C, Teixeira A, Oñate C, *et al.* Tumor-produced Interleukin-8 attracts human myeloid-derived suppressor cells and elicits extrusion of neutrophil extracellular traps (nets). *Clin Cancer Res* 2016;22:3924–36.
- 54 Opfermann P, Derhaschnig U, Felli A, *et al.* A pilot study on reparixin, a CXCR1/2 antagonist, to assess safety and efficacy in attenuating ischaemia-reperfusion injury and inflammation after on-pump coronary artery bypass graft surgery. *Clin Exp Immunol* 2015;180:131–42.
- 55 Nair P, Gaga M, Zervas E, *et al.* Safety and efficacy of a CXCR2 antagonist in patients with severe asthma and Sputum neutrophils:



a randomized, placebo-controlled clinical trial . *Clin Experimental*

Allergy 2012;42:1097–103.